Deformation behavior of laser bending of circular sheet metal

Q. Nadeem* **and S. J. Na**

Department of Mechanical Engineering, KAIST, Yuseong-Gu, Daejeon, South Korea

**Corresponding author: engr.nadeemqaiser@gmail.com*

Received October 26, 2010; accepted January 3, 2011; posted online April 18, 2011

The application of a thermal source in non-contact forming of sheet metal has long been used. However, the replacement of this thermal source with a laser beam promises much greater controllability of the process. This yields a process with strong potential for application in aerospace, shipbuilding, automobile, and manufacturing industries, as well as the rapid manufacturing of prototypes and adjustment of misaligned components. Forming is made possible through laser-induced non-uniform thermal stresses. In this letter, we use the geometrical transition from rectangular to circle-shaped specimen and ring-shaped specimen to observe the effect of geometry on deformation in laser forming. We conduct a series of experiments on a wide range of specimen geometries. The reasons for this behavior are also analyzed. Experimental results are compared with simulated values using the software ABAQUS. The utilization of line energy is found to be higher in the case of laser forming along linear irradiation than along curved ones. We also analyze the effect of strain hindrance. The findings of the study may be useful for the inverse problem, which involves acquiring the process parameters for a known target shape of a wide range of complex shape geometries.

OCIS codes: 140.0140, 160.0160.

doi: 10.3788/COL201109.051402.

Forming techniques consist of metal working processes in which the material is shaped in solid state by plastic deformation. There are two classifications of forming techniques: bulk forming and sheet forming. Bulk forming comprises rolling, extrusion, and forging. On the other hand, bending and contouring are common processes of sheet forming. Conventionally, sheet metal bending using punch and die requires hard tooling, external forces, and spring back action. The idea of using lasers for forming sheet metal was first conceived by Kitamura in Japan[1]. The laser forming process is concerned with the bending and correction of sheet metals/tubes using a laser beam. Laser forming of sheet metal components and tubes requires no hard tooling and external forces, and is therefore suited for die-less rapid prototyping and low-volume, high-variety production of sheet metal and tube components. Moshaiov *et al.*[2] showed that the process was similar to the well established torch flame bending used on large sheet material in the ship-building industry, but it offered much more control over the final product.

In recent years, laser forming techniques have been investigated extensively. Empirical, analytical, and finite element method (FEM) tools[3,4] have been used to predict the distortions and relation between bending angle and process parameters, such as power of the laser beam, speed at which the laser beam scans the sheet metal, and the laser beam spot diameter, among others. Most researches have focused on the laser forming along linear irradiation paths and over rectangular plates. Different irradiation strategies have to be developed for the production of complex shaped parts (e.g., a spherical dome). A certain deformation can be obtained if the laser beam scans the sheet several times along the same path. Edwardson *et al.*[5] studied the forming process of saddle-shaped parts using five different scanning strategies. Their results showed that the warped deformation occurred because of the dissymmetry of laser irradiations.

The effect of processing parameters on the deformation is not simple because we change linear scanning paths to curved paths. Similarly, laser forming of the circular shape specimens have deformation behaviors different from rectangular shapes. Hennige proposed a path strategy for ring and circle segments, but the range of segment angle was limited and the work did not explain the reasons for using arbitrary paths to obtain dome shape[6]. Paths used do not provide information regarding the offset between successive laser scanning passes, which initiates the need for further understanding of the process of laser forming along curved irradiations and curved geometry as well.

In this letter, we present the change in deformation behavior during transition from linear to curved geometries and irradiations. A significant change of the process mechanisms and its dependencies on the part geometry can be ascertained. The forming of axis-symmetric shapes that include ring-shaped geometry and circle-shaped geometry is investigated and compared with rectangular-shaped geometry. Moreover, the effects of strain hindrance on the deformation are investigated. All the experimental results are compared with simulated values using the software ABAQUS.

Deformation behavior in the laser forming process is entirely dependent on heating and cooling cycles called thermal cycles. There are three well-known mechanisms discussed in deformation behaviors: temperature gradient mechanism (TGM), buckling mechanism (BM), and up-setting mechanism (UM). TGM is the most widely reported mechanism and can be used to bend sheet metal out of plane toward the laser. Figure 1 shows the experimental set up comprising a fiber laser, a three-axis

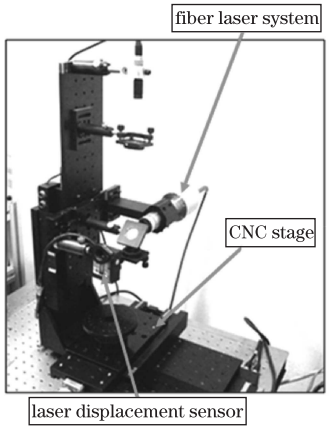

Fig. 1. Experimental Setup.

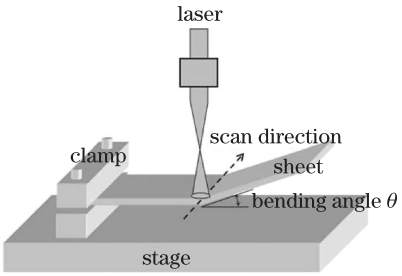

Fig. 2. Schematic of the laser bending setup.

computure numerical control (CNC) table, and a laser displacement sensor. The fiber laser used had a maximum power of 100 W and a motion assistant was used to control the three-axis CNC table.

If the specimen is not so large and the spot size is less than or nearly equal to the sheet thickness, the TGM mechanism is dominant for acquiring a given shape. Furthermore, the bending is always toward the laser beam, namely, positive bending (Fig. 2). We also apply positive bending with an adjustment of the process parameters in this study. The bending angle was measured by laser displacement sensor. To simplify the process, the velocity of laser scanning beam and radius of concentric heating paths r were kept constant at 720 mm/min and 30 mm, respectively, whereas the power of the laser beam P varied during the experiments otherwise stated. All specimens were made of common engineering low-carbon steel.

There were thus two basic part geometries, one of which can be considered as a circular plate having two radii (outer and inner radii), named ring-shaped specimen, and the other as a circular plate with an outer radius only, named circle-shaped specimen. The geometries mentioned above were selected to describe the transition from linear to curved irradiation laser bending. The circle-shaped specimens had a total radius of 50 mm, whereas the ring-shaped specimens had an outer radius of 50 mm and an inner radius of 10 mm. All specimens had a thickness of 0.8 mm. To enhance laser absorption by the workpiece, graphite coating was applied to the irradiated surface[7]. The segment angle β is defined as the total central angle of a specimen. This segment angle for a particular specimen is further subdivided into a number of small divisions called "in-plane angle α". Figure 3 illustrates three of the part geometries used in the experiments: Fig. 3(a) depicts circle-shaped specimen with $\beta = 90°$, Fig. 3(b) depicts ring-shaped specimen with $\beta = 90°$, and Fig. 3(c) depicts ring-shaped specimen with $\beta = 180°$. Radial lines along the circumferential direction show in-plane angles of 45°, 90°, 135°, and 180°, respectively. The objective of the in-plane angle is to measure the bending angle along the concentric heating path at a definite radius.

As a general rule, the minimum number of measuring locations or number of divisions of segment angle along the heating paths is three. To compensate for edge effects, the bending angle was not measured at or very close to the edges of specimens. The values of bending angles shown here were taken as the root-mean-square (RMS) average of measured angles at different in-plane angles. The time delay between any two consecutive passes was 90 s in case of multiple irradiations.

In addition to the geometries mentioned above, for comparison, rectangular plates acting as a reference base with varying segment angles were taken. These specimens were of constant length of 50 mm, whereas the width (heating source moving parallel to the width of plate) was equal to the length of concentric heating paths. One set of geometries for the segment angle of 90° is shown in Fig. 4. For instance, the width w of a referenced rectangular plate for definite segment angle is

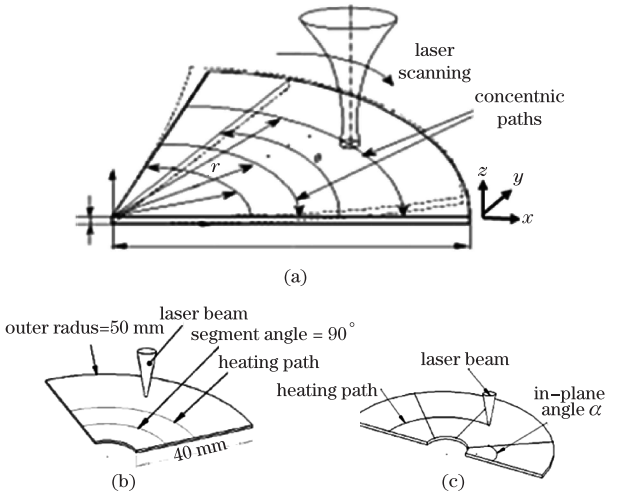

Fig. 3. Definition of circular part geometries, segment angle β, and in-plane angle α while concentric paths describe the heating path radius r_i. (a) Circle-shaped specimen, $\beta = 90°$; (b) ring-shaped specimen, $\beta = 90°$; (c) ring-shaped specimen, $\beta = 180°$.

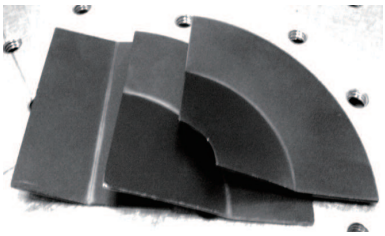

Fig. 4. Referenced rectangular, circle-shaped, and ring-shaped specimens (left to right), $\beta = 90°$, $r = 30$ mm.

defined as $w = r_i \times \beta_i$, where r_i is the radius of heating path, and β_i is the segment angle (in radians).

A specially designed jig that can rotate about the z-axis was used to facilitate accurate measurements.

A series of experiments for ring-shaped, circle-shaped, and referenced rectangular specimens were conducted for a range of $5° < \beta < 180°$. In addition to these experiments, a second series of investigations with constant $\beta = 180°$, $P = 80$ W, $r = 30$ mm, and varying inner radius from 0 to 25 mm were carried out.

If the sheet metal is relatively thin, the influence of strain hardening and material thickening along the bending edge is almost insignificant when the number of irradiations is small[8]. Hence, a linear relationship between bending angle and number of irradiations exists.

Figure 4 shows one set of formed specimens after experiments on the ring-shaped, circle-shaped, and referenced rectangular specimens. The laser had a spot diameter of 1 mm, and its power was maintained at a constant value of 80 W. Figure 5 clearly shows the influence of different irradiation geometries on the achievable bending angle for the case of multiple irradiations or number of passes (N).

As mentioned earlier, a series of experiments were conducted for all three kinds of specimens with different β values. Figure 6 shows some of the formed ring-shaped specimens, with $\beta = 45°$, 90°, 120°, and 180°. The overall bending angle was determined by the continuous heating and cooling events as well as the associated thermal effects[9]. The results of experiments are shown in Fig. 7. From the figure, the bending angle is clearly smaller for all specimens with $\beta = 5°$. This is because the surrounding cooled material is not sufficient to restrict the expansion of irradiated surface in the heating cycle. As a result, the material has the maximum counter bending, and during cooling cycles, the irradiated surface has comparatively less positive bending at the end of the forming process. When the segment angle increases up to 45°, the bending angle digressively increases for all three kinds of specimens. Different scanning methods showed different bending behaviors due to the dissimilar nature of factors affecting the deformation behavior. One important factor is geometrical constraint. Referenced rectangular specimens at particular segment angles have larger deformation than ring-shaped and circle-shaped specimens. This means that for linear irradiations, the maximum stresses utilized for deformation and the produced strains have an insignificant amount of strain hindrance. It was suggested that the line energy for linear irradiations is greater than that for curved irradiations[10]. Thus, deformations for linear irradiations are greater than those for curved irradiations. Another aspect has been described by Jung that during circular heating, strain histories exhibit greater thermal strain effect than plastic strain during heating[11]. Thus, the restraint or bending rigidity of the plate becomes non-symmetric, resulting in less bending angle. Hennige described the strong influence of the geometrical process induced strain hindrance on the forming results in the circle-line heating process[12]. The degree of the bend angle was digressive compared with the straight-line heating process. Other factors that have to be addressed might influence the residual stresses and change the forming mechanism itself. This behavior occurs at very early stages during forming, such as $\beta = 5°$.

In the case of referenced rectangular specimens, the bending angle continued to increase digressively up to a measured saturation value. On the other hand, for ring-shaped and circle-shaped specimens, $45° < \beta < 120°$, the bending angle decreased continuously. We also noticed that longitudinal distortion was induced when $\beta > 45°$. When $\beta > 120°$, the bending angle again started to increase for ring-shaped specimens but continued to decrease for circle-shaped specimens. For circle-shaped specimens, the strain hindrance had a strong negative effect on deformation. It implies that the complex mathematical analysis of combined effect of circumferential and radial stresses and longitudinal distortion is required.

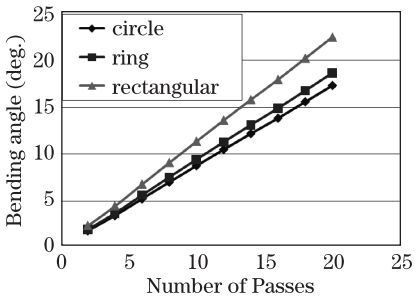

Fig. 5. Relation between bending angle and number of passes (N). $\beta = 90°$, $d = 1$ mm, $P = 80$ W.

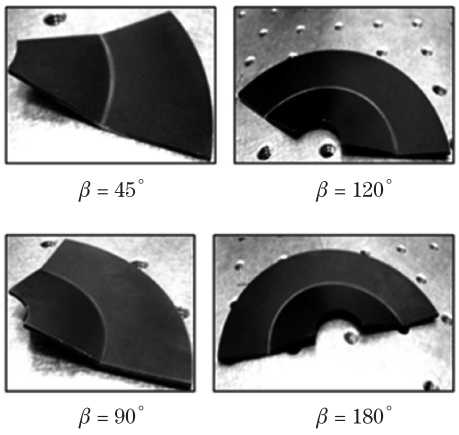

Fig. 6. Ring-shaped specimens after forming with $\beta = 45°$, 90°, 120°, and 180°.

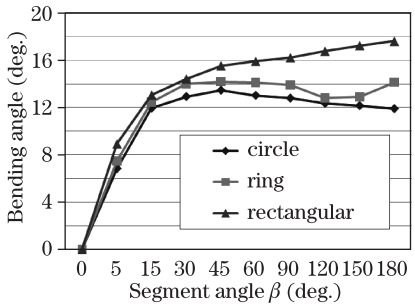

Fig. 7. Effect of transition geometries on deformation. $P = 80$ W, $N = 15$.

Among the ring-shaped and circle-shaped specimens, the latter has some additional amount of material near the inner side with varying influence along the circumference, which acts as a strong strain hindrance. If the strain hindrance is increased further using circle-shaped specimens instead of ring-shaped specimens, the achievable bending angle decreases in comparison with the corresponding ring-shaped specimens[6]. Therefore, circle-shaped specimens have smaller bending angles compared with ring-shaped specimens. If the inner radius of ring-shaped specimen is varied, it will have a negative or positive influence on deformation.

Experiments with a spot size of 1 mm, heating path-radius of 30 mm, and varying inner radius of ring-shaped specimens were carried out. Figure 8 describes the stated effect for half-circular ring-shaped specimen ($\beta = 180°$). The bending angle increases with increasing inner radius until edge effects dominate.

Zero value of the inner radius corresponded to the circle-shaped specimen. As shown in the figure, the bending angle decreases at an inner radius of 25 mm. Obviously, the reason for this was the edge effects because the heating path's radius of 30 mm and the inner radius of ring-shaped specimen of 25 mm were closer to each other. Therefore, the edge effects were significant.

FEM is a very strong and effective tool to study the laser forming process. The different stages of the process such as the developing of counter bending and the contraction during cooling could be identified with the use of FE simulations. Numerical simulation for curved irradiation paths on rectangular sheet and ring sheet metals has been studied[13,14]. The software used in this study for FE analysis was ABAQUS. A subroutine was also required for a simulation made in FORTRAN. It was a nonlinear, transient complex analysis that required simplifying assumptions, including the following aspects: 1) material is isotropic; 2) laser operates in continuous wave mode; 3) no melting occurs; 4) no external mechanical force exists; 5) variation of material parameters with temperature has been obtained by means of linear interpolation; 6) the metal plate is flat and free of residual stresses.

In the analysis, the heat source distribution was a Gaussian distribution. Furthermore, natural convection and radiation were used as boundary conditions for analysis. Process parameters similar to the actual process were also considered. Temperature-dependent thermal and mechanical material properties for low-carbon steel were taken from Ref. [7]. The temperature ranged

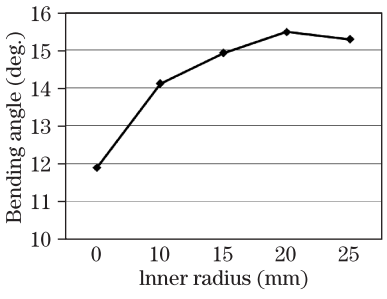

Fig. 8. Effect of strain hindrance at $\beta = 180°$. Bending angle increases with increasing inner radius until edge effects appear. Path radius is 30 mm, $P = 80$ W, $N = 15$.

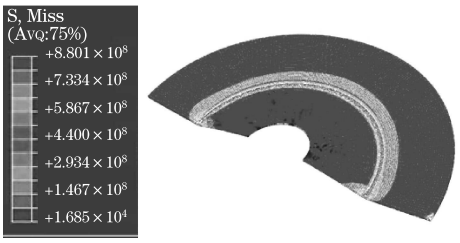

Fig. 9. FE simulation. Deformation is clearly toward the laser beam source. Ring-shaped specimen, $\beta = 180°$.

from 0 to 1400 °C with increments of 100 °C. All of the physical properties at any temperature can be determined by interpolation[3]. To ensure the quality of the analysis, unknown properties were considered through linear interpolation. These material properties were defined in ABAQUS program during the "defining material" stage[13].

FE analysis was sequential type, i.e., to conclude the deformation (structural analysis) behavior, output of thermal analysis was needed. Therefore, thermal analysis was finished before structural analysis. All the other process parameters considered in the FE analysis were similar with the ones used during experiments.

For verification of experimental results, a series of simulations was ran for ring-shaped specimens within the β range of 0°–180° and $N = 1$. Figure 9 shows the FE simulation model of ring-shaped specimen with $\beta = 180°$ only. The result after simulation clearly showed the deformation toward the laser beam.

As described above, the value of bending angle was the RMS average of values measured at various locations along definite concentric paths or in-plane angles. Figure 10 describes the validity of considered RMS value of bending angle. There is clearly a negligible deviation along the definite concentric path and experimental results match the FE simulation results. Additionally, for comparison, a series of numerical investigations was conducted for a number of ring-shaped specimens with $\beta = 0°$–180° at $N = 15$. Figure 11 illustrates the results of comparison between FE analysis calculations and experimental measured values. The deformation behavior during experiments indicates a very good correlation with FE investigations.

In conclusion, a series of investigation is carried out using experimental and numerical methods to analyze the influence of the curved irradiations and geometry transitions on deformation behavior in laser forming

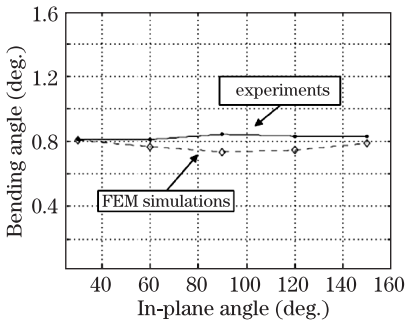

Fig. 10. Bending angle variation along definite concentric paths is insignificant as shown by experiments and FE simulation.

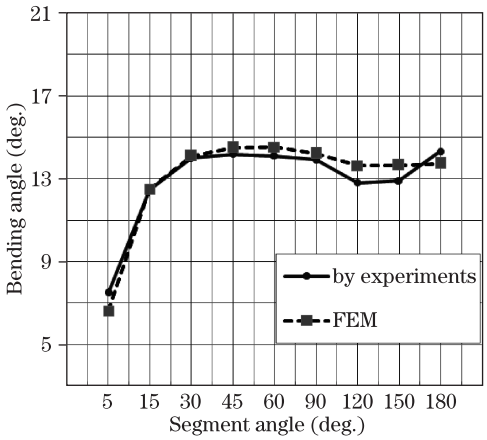

Fig. 11. Results of FE simulations and experiments have very good correlation, with negligible deviation, for ring-shaped specimens with $\beta = 0°$–$180°$.

process. Our investigations show that linear irradiation paths for rectangular plates have more deformation than curved irradiation paths for ring-shaped and circle-shaped specimens. This means that the utilization of line energy, and thus stresses for linear irradiations, is higher. Deformation along the particular concentric path has negligible deviation, which indicates the potential of curved irradiations for three-dimensional (3D) laser forming. The specimens having additional material near the center, such as the circle-shaped specimens, have less deformation than the ring-shaped specimens. The reason proposed is strain hindrance. FE analysis by ABAQUS software is found to be a very strong tool to predict the deformation behavior and provides very good correlation between numerically found and experimentally measured values of bending angles. To obtain improved understanding and control over the process, further study is needed. Future work will concentrate on the extension of β range from 0° to 360° and the handling of inverse problem to determine the process parameters for a given deformation or target shape for such kinds of geometries. Moreover, the influence of these underlying factors would be determined by utilizing numerical simulations under the laws of bending mechanics.

References

1. N. Kitamura, "Technical report of joint project on materials processing by high power laser" JWES-TP-8302 359 (1983).
2. A. Moshaiov and W. Vorus, J. Ship Res. **31,** 269 (1987).
3. Z. Ji and S. Wu, J. Mater. Process. Tech. **74,** 89 (1998).
4. A. K. Kyrsanidi, Th. B. Kermanidis, and S. G. Pantelakis, J. Mater. Process. Tech. **104,** 94 (2000).
5. S. P. Edwardson, K. G. Watkins, G. Dearden, and J. Magee, in *Proceedings of the 3rd International Conference on Laser Assisted Net Shaping* 559 (2001).
6. T. Hennige, J. Mater. Process. Tech. **103,** 102 (2001).
7. J. Kim and S. J. Na, Opt. Laser Technol. **35,** 605 (2003).
8. J. Bao and Y. L. Yao, J. Manuf. Sci. Eng. **123,** 53 (2001).
9. Z. Hu, R. Kovacevic, and M. Labudovic, Int. J. Machine Tools and Manufacture **42,** 1427 (2002).
10. Q. Nadeem, W. J. Seong, and S. J. Na, in *Proceedings of Autumn Annual Conference of KWJS* **52,** 22 (2009).
11. H. C. Jung, "A study on laser forming processes with finite element analysis" PhD. Thesis (University of Canterbury, Christchurch, 2006).
12. T. Hennige, in *Proceedings of the LANE'97* 409 (1997).
13. P. Zhang, J. Yu, and X. Zheng, Tsinghua Sci. Technol. **14,** 132 (2009).
14. P. Zhang, B. Guo, D. B. Shan, and Z. Ji, J. Mater. Process. Tech. **184,** 157 (2007).